1. Introduction

Since the beginning of the information age in the 1960s, the development of magnetic storage devices played the decisive role for the advancements in computer technology. The importance of this core technology for the digital revolution is equivalent with that of the silicon transistor, firstly developed by Morris Tanenbaum in 1954 [Tan55]. Only an ongoing miniaturization and increase in storage density was capable to keep up with the needs of digitalization in all areas of life [Plu12]. It was only in the last several years that the solid-state drive (SSD), which is based on integrated circuits and semiconductor technology, gained importance as a mass storage medium because of its speed advantage. In terms of storage size, reliability, and price per data volume, however, the SSD cannot compete with a magnetic hard disk drive (HDD). In these respects the HDD is still the first choice.

The basic function principle of a HDD has not been changed over decades. A circular disk coated with a ferromagnetic material rotates beneath a coil which serves as a switchable electromagnet. The magnetic field of this coil aligns the magnetization of microscopic areas, the so-called domains, along one of two opposite directions. These domains represent the bits as the smallest units of digital information. Nevertheless, during the process of miniaturization many issues had to be solved. The most noteworthy discovery is for sure the giant magnetoresistance (GMR) [Bai88, Bin89] which resulted in a dramatical increase of the sensitivity of the reading sensors and allows for much smaller domains. This importance was eventually honored with the Nobel Prize in Physics for Albert Fert and Peter Grünberg in 2007. It also demonstrates that new surprising discoveries are still possible in the field of magnetism and may have a huge impact on technology. Today the use of perpendicular magnetic recording makes it possible to realize even higher densities of the data.

Although the hard disk drive concept has proven itself over half a century, the two major problems, namely liability of the mechanical parts and non-addressability of individual bits, are still an issue. The information has to be read sequentially from large blocks limiting the speed of data access. This is in contrast to random-access memory where in principle every data cell can be accessed directly. Originally this range of application was covered by transistor-based devices which store the information in form of electrical charges. Today magnetoresistive random-access memory (MRAM), which again uses the magnetization for storage, is believed to combine the speed advantage of direct access with the nonvolatility of conventional magnetic recording. The spin-transfer induced switching of magnetic cells is the latest advancement currently in development. Instead of using the magnetic field accompanying high electrical currents for the switching of data bits, the torque of a much smaller spin-polarized current is used for the writing process. This reduces not only the power consumption but also allows for

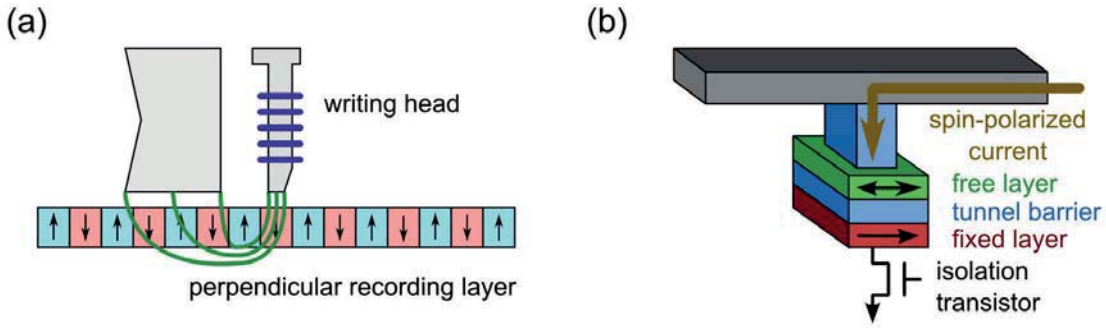

Figure 1.1.: Illustration of state-of-the-art magnetic recording and storage media. (a) Hard disk drive using perpendicular recording. The perpendicularly magnetized media allows for a much higher data density than the conventional in-plane type. The disk rotates beneath the writing head which focuses the magnetic field lines in order to switch single domains. (b) Single data cell of a spin-torque magnetoresistive random-access memory (ST-MRAM). A spin-polarized electrical current exerts a torque on the the free layer and switches its magnetization. For the reading process the cell serves as a magnetic tunnel junction. The illustration is modified from Ref. [Eve14].

much higher element density because of lower crosstalk. At the same time the cell serves as a magnetic tunnel junction that makes use of the tunnel magnetoresistance (TMR) effect [Jul75, Miy95] for the purpose of reading and the identification of the magnetic state. Figure 1.1 illustrates two different state-of-the-art concepts for magnetic data storage.

Another recently proposed concept for an MRAM is the vortex random access memory (VRAM) [Boh08]. It uses a combination of alternating magnetic fields and spin-polarized currents to switch the state of a special magnetic domain pattern [Wae06], the so-called magnetic vortex. These vortices occur in ferromagnetic microstructures resembling a disk, and are characterized by a curling of the magnetization around a core. The direction of this vortex core and the sense of curling can be controlled independently. By that one single disk can represent even four different states which is equivalent to two bits of information. Furthermore, the magnetic vortex shows unique high-frequency dynamics [Cho04] studied intensely. Several concepts for the selective manipulation of the vortex state, including rotational excitation [Kra07, Kim08], picosecond excitation by spin-waves [Kam11, Kam12], or out-of-plane currents [Cho10] have been presented.

All these concepts motivate a detailed investigation of magnetic vortices under the influence of magnetic fields and spin currents, which is the main topic of this thesis. In addition we study the topological counterpart, the magnetic antivortex, that has not attracted much attention to date but shows a similar dynamic behavior [Wan07] and could also be used for data-storage devices [Dre09]. Many publications are limited to one single method of investigation. Here we present a comprehensive study that includes the combination of different experiments, theoretical descriptions, as well as micromagnetic simulations. As one experimental method we use the time-resolved x-ray microscopy available at synchrotron-light sources, such as the Advanced Light Source in Berkeley, CA, USA and BESSY II, Berlin, Germany. It offers a unique possibility to directly image the vortex dynamics at its genuine time and length scales.

We develop a profound understanding which is supported by broadband ferromagnetic absorption spectroscopy that gives the response in the frequency domain.

This work is structured as follows: in chapter 2 we recapitulate the theoretical background that is necessary for the understanding of vortex dynamics as well as the experimental techniques. The latter are presented in chapter 3. Furthermore, we give an overview on the computational methods, with a focus on the numerical solution of the micromagnetic equations. Although these are known for many decades [Lan35], only the advancement of computational power in the last twenty years enabled an accurate simulation of the micron-sized structures investigated in this work. This is followed by a detailed description of the experimental setups used for x-ray microscopy and ferromagnetic absorption spectroscopy. Our results are presented in chapter 4. We begin with a comprehensive analytical model in Sec. 4.1, that describes the excitation of magnetic vortices and antivortices by two-dimensional fields and spin-currents. The model is applied to the special case of rotational excitation. For antivortices this calculation results in a surprising asymmetric coupling to the two driving forces. We use micromagnetic simulations and time-resolved x-ray microscopy for the verification of these main findings. In a second part, Sec. 4.2, we present experimental results that clearly show deviations from the model derived in the first part. This motivates us to introduce additional nonlinear extensions. A detailed understanding of these aspects is the key for a successful application of vortices for data storage, as presented above. The extensions include nonparabolic and anisotropic confining potentials as well as a critical limit for the vortex velocity. Finally, the presentation of our results closes with a conclusion in chapter 5. Most of the work presented is published in articles of peer-reviewed journals. We concentrate on the results of four publications. A full list of publications is found in appendix D.

2. Theoretical background

This chapter deals with the descriptions of ferromagnetism in magnetic microstructures. The theoretical background presented here is important for the understanding of the methods employed in this work and for the analysis of the experimental data. We start with a short explanation of the quantum-mechanical origin of ferromagnetism in Sec. 2.1. In Sec. 2.2 we limit our considerations to the micromagnetic model, which is capable of describing ferromagnetism on a micrometer length scale. We present the energy contributions that affect the static and dynamic behavior of nanomagnets. The Landau-Lifshitz-Gilbert equation and the Thiele equation are introduced as the equations of motion of the magnetization. They are extended to account for the influence of spin-polarized electrical currents. The last section 2.3 discusses the magnetic circular dichroism, which is observed for x-ray light absorbed by ferromagnets and which is used for time-resolved measurements of the magnetization dynamics in this work.

2.1. Magnetism in solids

The magnetization $\mathbf{M}$ of a solid is defined as the magnetic moment per volume. External magnetic fields $\mathbf{H}$ interact with the magnetic moments of atoms or can induce these moments in the first place. Depending on whether these atoms have intrinsic magnetic moments or there are interactions between neighboring atoms, there are several phenomena that have to be distinguished. These differ in the behavior of the magnetic induction $\mathbf{B}$ that is proportional to the sum of magnetic field and magnetization:

$$\mathbf{B} = \mu_0 \left(\mathbf{H} + \mathbf{M} \right), \tag{2.1}$$

where $\mathbf{H}$ and $\mathbf{M}$ are measured in units of ampere per meter, and $\mathbf{B}$ in units of tesla with $1\,\mathrm{T} := 1\,\mathrm{V\,s\,m^{-2}}$. Also $\mu_0 = 4\pi \times \mathrm{V\,s\,A^{-1}\,m^{-1}}$ is the magnetic permeability of the vacuum. In vacuum where no magnetic moments are present ($\mathbf{M} = 0$), Eq. 2.1 simplifies to $\mathbf{B} = \mu_0 \mathbf{H}$. This is also a good approximation for most gases, in particular for air.

In solids, however, there are induced or inherent magnetic moments ($\mathbf{M} \neq 0$) that interact with the magnetic field $\mathbf{H}$. So these two fields are not independent of each other. To describe their relation we define the dimensionless magnetic susceptibility χ by:

$$\mathbf{M} = \chi\, \mathbf{H}\,. \tag{2.2}$$

Inserting this into Eq. 2.1 we also get the relation between magnetic induction and magnetic field:

$$\mathbf{B} = \mu_0 \left(\mathbf{H} + \chi\, \mathbf{H} \right) = \mu_0 \left(1 + \chi \right) \mathbf{H} = \mu\, \mu_0\, \mathbf{H}\,, \tag{2.3}$$

characterized by the relative magnetic permeability $\mu = 1 + \chi$.

Diamagnetism and paramagnetism:
Every single electron of an atom's electron shell possesses a magnetic moment. The overall magnetic moment of the electron configuration is determined by the Pauli exclusion principle and Hund's rules. In the case of a diamagnetic material the magnetic moments inside the electron shell compensate each other, so that the atom has no effective magnetic moment. Nevertheless, an external magnetic field always induces a small magnetic moment that is proportional but antiparallel to this field. The magnetic susceptibility χ becomes a scalar quantity with:

$$\chi < 0 \qquad \Longrightarrow \qquad \mu = 1 + \chi < 1 \qquad \text{(diamagnetism)}. \tag{2.4}$$

By that also the magnetic induction $\mathbf{B}$ is proportional to the magnetic field but slightly reduced compared to the vacuum case. Every material shows a diamagnetic behavior that is often overcome by other magnetic properties.

In the case of paramagnetism the magnetic moments of the electrons do not compensate each other and the atoms hold finite magnetic moments. These moments are not coupled and thus disordered but can be aligned in parallel when an external field is applied. This results once more in a magnetization proportional to $\mathbf{H}$, but now with positive scalar susceptibility and a relative permeability greater than one, respectively:

$$\chi > 0 \qquad \Longrightarrow \qquad \mu = 1 + \chi > 1 \qquad \text{(paramagnetism)}. \tag{2.5}$$

The magnetic induction is increased compared to the case of the vacuum. An example are the alkali metals with only one s-electron that gives a large contribution to the permeability. The disorder of the moments strongly depends on temperature, making $\chi(T)$ and $\mu(T)$ temperature-dependent functions.

Ferromagnetism:
In ferromagnetic materials the magnetic moments are not independent but spontaneously align parallel to each other inside of small regions, the so-called magnetic domains. The origin of ferromagnetism is the quantum mechanical electron exchange, that bases on the Pauli principle and the Coulomb repulsion of two electrons [Sto06]. Even in one of the simplest two-electron system, the helium atom, these give rise to a splitting into singlet and triplet states with different alignment of the spins and energies.

Inside a solid the electron exchange is often illustrated using the simple ansatz of the Heisenberg model [Hei28]. Assuming parallel or antiparallel alignment of N electron spins, the effective Heisenberg Hamiltonian is given by:

$$\hat{H}_{\text{eff}} = -2 \sum_{i<j}^{N} J_{ij}\, \hat{s}_i \cdot \hat{s}_j \,. \tag{2.6}$$

Here $\hat{s}_{i,j}$ are the spin operators and J_{ij} is the exchange integral with:

$$J_{ij} = \int\int \Phi_i(\mathbf{r_1})\, \Phi_j(\mathbf{r_2})\, \frac{e^2}{4\pi\, |\mathbf{r_2} - \mathbf{r_1}|} \Phi_i^*(\mathbf{r_2})\, \Phi_j^*(\mathbf{r_1})\, dr_1^3 dr_2^3 \,. \tag{2.7}$$

$\Phi_{i,j}$ are the single electron wave functions. For ferromagnetic coupling J_{ij} is positive and the energy of the system is lowered for a parallel configuration of the spins.

The Heisenberg model assumes localized spins. In the ferromagnetic 3d-transition metals (Fe, Co, Ni) and their alloys, however, the magnetic moment is carried by the 3d electrons. The latter are delocalized since the periodicity of the crystal lattice causes the formation of a band structure for these 3d electrons. Nevertheless these bands are energetically split due to the exchange interaction and differently occupied. The unequal amounts of majority and minority spins results in an averaged net magnetic moment [Sto06].

Due to the formation of magnetic domains the relation between the magnetic field and the magnetization of a solid is much more complicated than in the case of diamagnets and paramagnets. In particular the magnetization inside one of these domains is several orders of magnitude greater and its absolute value is a material specific constant:

$$\mathbf{M}(\mathbf{r}) = M_\mathrm{S}\,\mathbf{m}(\mathbf{r})\,. \tag{2.8}$$

Here M_S is the so-called saturation magnetization and the unit vector $|\mathbf{m}| = 1$ gives the direction of the magnetization inside of the domain with position $\mathbf{r}$. The averaged magnetization depends on the shape, size and direction of the magnetic domains and does not have to be in parallel with the magnetic field. Furthermore it depends on the history of the applied field and on additional anisotropies that favor specific directions for alignment (e.g. the magneto-crystalline anisotropy). In the most common case only a differential susceptibility can be defined as a 3×3 tensor that consists of the partial derivatives of $\mathbf{M}$ with respect to the components of $\mathbf{H}$. By that the differential susceptibility describes the change of magnetization for a distinct infinitesimal variation of the magnetic field. A typical hysteresis curve of a macroscopic ferromagnetic body is shown in Fig. 2.1. For soft-magnetic materials with low anisotropies the coercive field is small and the hysteresis loop is almost closed.

2.2. Micromagnetic model and Landau-Lifshitz equation

As mentioned in Sec. 2.1, the behavior of the magnetization in macroscopic ferromagnetic bodies is complicated but can be described very well neglecting the exact underlying microscopic processes. The magnetization is represented by only one averaged "macro spin" for the whole body. While this description is valid for magnetic samples in the millimeter range and above, it cannot be applied for magnetic microstructures where the dimensions go down to the size of a few or single domains. In this intermediate range also the atomic theory is not applicable because of the vast number of single spins that have to be considered.

Because magnetic microstructures are the main focus of this thesis, we will concentrate on a model that can describe the static states as well as the dynamics of the magnetization in this intermediate range. This model is called the *Micromagnetic Model* and is based on the treatment of the magnetization as a continuous vector

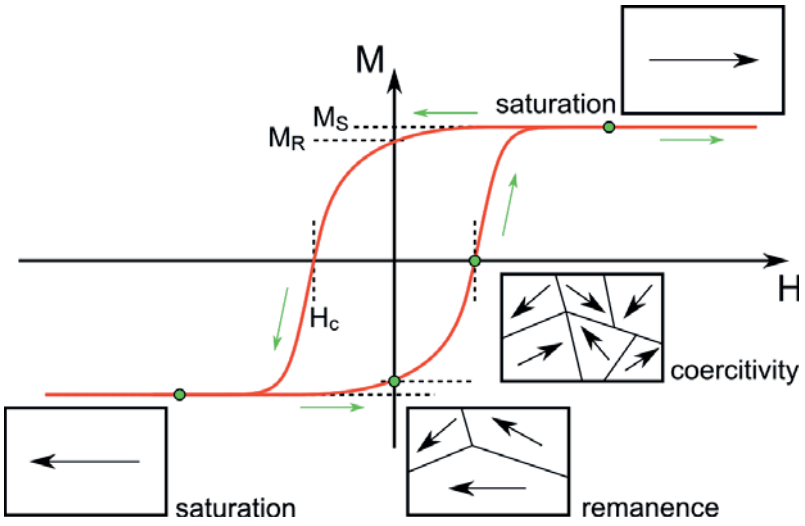

Figure 2.1.: Hysteresis curve of a macroscopic ferromagnetic body. The projection M of the magnetization is plotted against the magnitude H of the applied field. In saturation all domains are aligned parallel to the magnetic field. Because of anisotropies the domains maintain this direction also at zero field, resulting in a averaged remanence magnetization M_{R}. To demagnetize the body a coercitive field H_{C} with reversed direction has to be applied.

field $\mathbf{M}(\mathbf{r})$, that is in contrast to the two approaches mentioned above. This vector field is connected to a set of micromagnetic energies and fields that abstract the quantum-mechanical origin of ferromagnetism. Following the variation principle one can derive an equation of motion for the magnetization known as the Landau-Lifshitz equation. The micromagnetic energies that are needed to explain the behavior of soft ferromagnetic materials are shown in the following. Subsequently we will introduce the Landau-Lifshitz equation and the derived Thiele equation that describes the motion of entire magnetization patterns as a rigid particle.

2.2.1. Exchange energy

The Heisenberg Hamiltonian $\hat{H}$ describes the interaction of localized and neighboring spins only. To adopt this model to the continuum one can expand it into a Taylor series. A similar approach can be found e.g. in references [Kit49] and [Blu01]. We start with the Heisenberg Hamiltonian, where the exchange integral J of two spins $\mathbf{S_i}$ and $\mathbf{S_j}$ is positive for ferromagnetic materials:

$$\hat{H} = -J\,\mathbf{S_i}\cdot\mathbf{S_j} = -JS^2\,\cos\Phi_{ij} \tag{2.9}$$

For small angles Φ_{ij} between the spins we can expand the cosine using $\cos x \approx 1 - \frac{x^2}{2}$ and derive:

$$\hat{H} = -JS^2 + \frac{JS^2}{2}\Phi_{ij}^2\,, \tag{2.10}$$

where the first term can be neglected because it is constant and gives an offset energy only.

For simplification we now assume a cubic lattice where the lattice constant a equals the nearest neighbor distance. The volume of the unit cell is a^3. According to Eq. 2.10 the energy density ε_{ij} inside of one single cell is then given by:

$$\varepsilon_{ij} = \frac{JS^2}{2\,a^3}\Phi_{ij}^2 \,. \tag{2.11}$$

We now make the continuum approximation for the magnetization $\mathbf{m}$ using $\Phi \approx |(\mathbf{a}\cdot\nabla)\,\mathbf{m}|$ and derive an energy density of:

$$\varepsilon_{\text{exch}} = A\cdot\left[(\nabla m_x)^2 + (\nabla m_y)^2 + (\nabla m_z)^2\right] \qquad \text{with} \qquad A = \frac{JS^2}{2\,a}\,. \tag{2.12}$$

The exchange constant A is a material specific parameter and the exchange energy E_{exch} of the entire magnetic body is given by the integration of $\varepsilon_{\text{exch}}$ over the body's volume V:

$$E_{\text{exch}} = A\int_V (\nabla m_x)^2 + (\nabla m_y)^2 + (\nabla m_z)^2 \; dr^3\,. \tag{2.13}$$

In literature the term $(\nabla m_x)^2 + (\nabla m_y)^2 + (\nabla m_z)^2$ is often shortened by $(\nabla\mathbf{m})^2$, that has not to be confused with the squared divergence of $\mathbf{m}$. We see that inhomogeneities of the magnetization cause the exchange energy to increase. For a homogeneously magnetized body the gradients of the components of $\mathbf{m}$ equal zero everywhere and the exchange energy in minimal. The exchange energy is called a *local* energy because its density depends only on the local magnetization. Its calculation is thereby rather trivial.

Because the exchange energy favors a parallel alignment of neighboring magnetic moments their direction can only change slowly over a finite distance. This characteristic length depends on additional energy contributions. In soft-magnetic materials without anisotropies we can restrict to magnetostatic interactions which results in the magnetostatic exchange length l_{S}:

$$l_{\text{S}} = \sqrt{\frac{2A}{\mu_0 M_{\text{S}}^2}}\,. \tag{2.14}$$

For the alloy $Ni_{80}Fe_{20}$ (permalloy) we find $l_{\text{S}} \approx 5\,\text{nm}$. This serves as a lower limit for magnetic inhomogenities such as domain walls or magnetic vortices which are discussed in this work.

2.2.2. Zeeman energy

The Zeeman energy E_{z} describes the interaction of the magnetization $\mathbf{M}$ with an external field $\mathbf{H}_{\text{ex}}$ [Hub98]:

$$E_{\text{z}} = -\mu_0\int_V \mathbf{M}\cdot\mathbf{H}_{\text{ex}}\,d^3r\,. \tag{2.15}$$

This energy is minimized by the parallel alignment of the magnetization to the applied field. If $\mathbf{H}_{\text{ex}}$ is large enough to overcome all other contributions to the total energy the magnetic structure can be saturated in the given direction.

2.2.3. Demagnetization energy

The demagnetization energy arises from the interaction with a magnetic field, that is generated by the magnetization distribution itself. The origin of this field is directly connected to Gauss's law for magnetism (Maxwell's second equation) which reads:

$$\nabla \cdot \mathbf{B} = 0\,. \tag{2.16}$$

The magnetic induction $\mathbf{B}$ is a divergence free vector field. Thus, it possesses no sources or sinks: it is solenoidal. Another often used description is that magnetic monopoles do not exist. This can be somehow confusing. Although this statement is true for the magnetic induction $\mathbf{B}$, it does not hold for the magnetic field. By comparing Eq. 2.16 with Eq. 2.1 we derive in the absence of external magnetic fields:

$$\begin{aligned} \nabla \cdot \mathbf{B} &= \mu_0 \nabla \cdot (\mathbf{H}_\mathrm{d} + \mathbf{M}) = 0 \\ \Leftrightarrow \qquad \nabla \cdot \mathbf{H}_\mathrm{d} &= -\nabla \cdot \mathbf{M}\,. \end{aligned} \tag{2.17}$$

Since the magnetic induction has to be solenoidal, the sinks of the magnetization are compensated by the sources of a magnetic field. This is called demagnetization field $\mathbf{H}_\mathrm{d}$ inside the ferromagnet and stray field in the outside. The inverse case is valid as well: the sources of $\mathbf{M}$ are the sinks of $\mathbf{H}_\mathrm{d}$.

Furthermore, Ampère's law states that the magnetic field is irrotational ($\nabla \times \mathbf{H} = 0$) in the absence of electrical currents. Every irrotational vector field can be described as the gradient of a scalar potential, so we can define the magnetostatic potential Φ_d:

$$\mathbf{H}_\mathrm{d} = -\nabla \Phi_\mathrm{d}\,. \tag{2.18}$$

By inserting this into Eq. 2.17 we get Poisson's equation for the magnetostatic potential:

$$\Delta \Phi_\mathrm{d} = -\left(\rho_\mathrm{V} + \sigma_\mathrm{S}\right)\,, \tag{2.19}$$

where the magnetic volume charges ρ_V and magnetic surface charges σ_S are defined by [Mil07]:

$$\rho_\mathrm{V} = -\nabla \cdot \mathbf{M} \qquad \text{and} \qquad \sigma_\mathrm{S} = \mathbf{M} \cdot \mathbf{n} \quad . \tag{2.20}$$

Here, $\mathbf{n}$ is the normal vector of the surface. The definition of magnetic surface charges takes into account, that the divergence is not defined on the surface of a magnetic body. Furthermore, all magnetic charges sum up to zero. The calculation of the magnetostatic potential is completely analogous to the problem of the electrostatic potential Φ_el and electrical charges ρ_el. The solution of Eq. 2.19 is given by:

$$\Phi_\mathrm{d}(\mathbf{r}) = \frac{1}{4\pi}\left[\int_V \frac{\rho_\mathrm{V}(\mathbf{r}')}{|\mathbf{r}-\mathbf{r}'|}\,d^3r' + \oint_{\partial V} \frac{\sigma_\mathrm{S}(\mathbf{r}')}{|\mathbf{r}-\mathbf{r}'|}\,d^2r'\right]\,. \tag{2.21}$$

Using the identity

$$\nabla \frac{1}{|\mathbf{r}-\mathbf{r}'|} = \frac{\mathbf{r}-\mathbf{r}'}{|\mathbf{r}-\mathbf{r}'|^3} \tag{2.22}$$